Peroxydisulfate activation by CuO pellets in a fixed-bed column, operating mode and assessments for antibiotics degradation and urban wastewater disinfection

Chan Li, Nayara de Melo Costa Serge, Raquel Fernandes Pupo Nogueira, Serge Chiron, Vincent Goetz

Peroxydisulfate activation by CuO pellets in a fixed-bed column, operating mode and assessments for antibiotics degradation and urban wastewater disinfection

Chan Li[1], Nayara de Melo Costa Serge[2], Raquel Fernandes Pupo Nogueira[2], Serge Chiron[1], and Vincent Goetz[3*]

[1]UMR5151 HydroSciences Montpellier, University of Montpellier, IRD, 15 Ave Charles Flahault 34093 Montpellier cedex 5, France

[2] São Paulo State University (UNESP), Institute of Chemistry, Araraquara, 14800-900, Araraquara (SP), Brazil

[3]PROMES-CNRS UPR 8521, PROcess Material and Solar Energy, Rambla de la Thermodynamique, 66100 Perpignan, France

*Corresponding author: Tel: + 33 - 468682236; Fax: + 33 - 468682213; e-mail address: vincent.goetz@promes.cnrs.fr

Abstract

A fixed-bed column packed with copper oxide pellets (FBC-CuO) combined with peroxydisulfate (PDS) as a primary oxidant was assessed as an option for simultaneously wastewater decontamination (antibiotics) and disinfection (bacteria, viruses, and protozoa). Preliminary to these experiments, phenol was used as the target molecule to investigate the working mode of FBC-CuO under various operating conditions, such as varying flow rates, initial persulfate and phenol concentrations. Then, the removal of a mix of five representative antibiotics (amoxicillin (AMX), cefalexin (CFX), ofloxacin (OFL), sulfamethoxazole (SMX), and clarithromycin (CLA)) in secondary treated urban wastewater (STWW) was evaluated. AMX, CFX, and OFL were effectively removed by simply flowing through the FBC-CuO, and the addition of PDS (500 µM) systematically enhanced the degradation of all targeted antibiotics, which is also the necessary condition for the removal of SMX and CLA. Urban wastewater disinfection was evaluated by monitoring targeted pathogens originally in the STWW. A significant reduction of *E. coli*, *Enterococcus*, *F-specific RNA bacteriophages* was observed after the treatment by FBC-CuO with 500 µM PDS. X-ray diffraction measurement and scanning electron microscopy performed on CuO pellets before and after treatment confirmed that the structure of the catalyst was preserved without any phase segregation. Finally, quantification of Cu(II) at the outlet of FBC-CuO indicate a non-negligible but limited released. All these results underline the potential of the FBC-CuO combined with PDS at the field scale for the degradation of micropollutants and inactivation of pathogens in wastewater.

Keywords: Fixed-bed column; copper oxide pellet; operating parameters; antibiotics; disinfection; secondary treated wastewater

1. Introduction

Conventional urban wastewater treatment plants are poorly effective to comprehensively remove most organic micropollutants, pathogens, as well as antibiotic resistance genes (Ternes et al. 2017; Rizzo et al. 2020). The occurrence and the large discharging amounts of these contaminants in municipal wastewater is a concern due to its potential ecotoxicological and hazardous effects on receiving nature waters or reclaimed wastewater reuse (Wang et al. 2020). Therefore, effective additional treatment steps for micropollutants degradation, pathogens inactivation, as well as antibiotic resistance reduction are required.

Advanced oxidation processes (AOPs) employing hydrogen peroxide and persulfate have been seen as a promising technology for water decontamination and disinfection simultaneously, which rely on radical and non-radical reactive species produced by activating oxidants, such as sulfate radicals ($SO_4^{\cdot-}$), singlet oxygen ($^1O_2$), and high valent metal ions (Waclawek et al. 2017; Lee et al. 2020; Rizzo et al. 2020; Chen et al. 2021). Oxidants activation can be achieved by an input of energy (UV, heat), electrolysis, transition metal ions, metal oxides, carbon materials, etc. (Wang and Wang 2018; Brienza et al. 2019; Lee et al. 2020). However, the high cost of the required extra energy, the recycling difficulty of metal ions limit their application. In an attempt to overcome these disadvantages, heterogeneous Fenton-like processes using different recyclable solid catalysts, such as iron oxides (Yan et al.2011; Obra et al. 2020; Luo et al. 2021) or copper oxide (CuO) (Du et al 2017; Ding et al. 2022), have been developed recently, and have shown high decontamination and disinfection capacity.

Among them, the CuO activated peroxydisulfate (PDS) system is an attractive option for potential application in organic matters enriched urban wastewater treatment (Zhang et al. 2014; Du et al 2017; Li et al. 2021; Ding et al. 2022; Li et al. 2022) due to the mild non-radical activation pathways combined with the highly selective reactive species production. The mechanisms of organic compounds degradation and pathogens

inactivation by the CuO/PDS system have been investigated in details by previous studies (Liang et al. 2013; Zhang et al. 2014; Du et al 2017; Cho et al. 2020; Zhou et al. 2020). Specifically, in the recent studies of our research group carried out in batch operating mode, in beaker, with micro-sized particles (Li et al. 2021; Li et al. 2022), the CuO/PDS system has been confirmed as effective for degradation of organic pollutants (i.e., phenol and several antibiotics), inactivation of pathogens and antibiotic resistant-bacteria and resistance genes. Cupryl ion (Cu(III)) was highlighted as the predominant reactive species, which could selectively oxidize the electron-rich phenolic amino acids, antibiotics (i.e., cefalexin, ciprofloxacin, sulfamethoxazole, and clarithromycin), as well as guanine and L-tyrosine, thus causing damages to the DNA and protein of bacteria and viruses.

With a mid-term perspective of large scale applications, the study of CuO/PDS systems carried out in fixed bed column operating in open and continuous flow is a relevant step. Although already tested in the case of micro-sized particles for 2,4-dichlorophenol degradation (Zhang et al. 2014) and nanoparticles supported on alumina granules for virus removal evaluation (Mazurkow et al. 2020), this option has received very few attentions in the literature. Thus, even if processes based on fixed-bed column are very well known in chemical engineering and well identified to provide efficient components separation by catalytic treatment or chemical reactions (Levenspiel 1972, Crittenden et al. 2012; Andrigo et al. 1999), there are still a lot of unknowns about the working mode and performances of a CuO/PDS advanced oxidative system operating according a packed bed principle.

The objectives of this paper is to provide first experimental trials of PDS activation for antibiotics degradation and urban wastewater disinfection with a fixed-fed column filled with millimetric CuO pellets (FBC-CuO). Prior to these tests, an extended experimental study was carried out in the case of a very basic effluent to be treated, that consisted of phenol in distilled water with Tris buffer (DW). Data were collected for

different operating parameters, such as the inflow PDS concentration or flow rate, to provide a clear and argued qualitative description of the operating mode of this process.

The most commonly used and frequently detected in the environment family of antibiotics in the world are the β-lactam antibiotics, including penicillins and cephalosporins. Amoxicillin (AMX) and cefalexin (CFX) are belongings to the aminopenicillin and cephalosporins family, which have been detected in raw sewage, effluents of sewage treatment plants, and even surface waters (Hirte et al. 2016; Qian et alk.2018). In addition to β-lactam antibiotics, sulfonamide, macrolide, as well as fluoroquinolone antibiotics are the most prominent classes of antimicrobial agents, with widespread usage in both human and veterinary medicines, which occurs ubiquitously in aquatic systems that are influenced by anthropogenic activities (Schönfeld et al. 1986; Gmurek et al. 2015; Poirier-Larabie et al. 2016; Senta et al. 2017). The evaluation of the antibiotics removal efficiency in DW and secondary treated waste water (STWW) was performed by using a mixture i.e. amoxicillin (AMX), cefalexin (CFX), ofloxacin (OFL), sulfamethoxazole (SMX), selected to cover a the broad spectrum of antibiotics families. The evaluation of STWW disinfection performance is assessed by using *Escherichia coli* (*E. coli*), *Enterococcus*, *F-specific RNA coliphages*, and *spores of sulfite-reducing bacteria* as pathogenic indicators. Catalyst stability evaluation by analyzing the Cu(II) leaching and comparing the morphology and crystallinity of CuO pellet before and after treatment complement the characterizations of the FBC-CuO process.

2. Experimental section

2.1 Chemicals

CuO pellet (> 99.9%) was purchased from Merck (Germany). Phenol, amoxicillin (AMX), cephalexin (CFX, > 99%), clarithromycin (CLA, > 99.9%), ofloxacin (OFL, > 99.9%), sulfamethoxazole (SMX, > 99.9%), potassium peroxydisulfate ($K_2S_2O_8$, > 99.9%), sodium thiosulfate (NaS_2O_3), and EDTA were purchased from Sigma-Aldrich

(Saint Quentin Fallavier, France). Potassium iodide (KI), potassium periodate (KIO_4), and tris(hydroxymethyl)aminomethane (Tris) were purchased from Merck KGaA (Germany). Acetonitrile (HPLC grade), methanol (MeOH, HPLC grade), and sodium chloride (NaCl) were purchased from Carlo Erba reagents (France). All the reagents used were of analytical grade and were used as received. Milli-Q water from a Direct-Q® system (Millipore) was used for the stock solution preparation and the HPLC analyses.

2.2 CuO pellets

The CuO pellets (0.7-2 mm) morphology was analyzed using JEOL 6490 scanning electron microscope (SEM). X-ray diffractometry (XRD) was performed using a Bruker D8 Advance in Bragg-Brentano geometry with a Cu source. Diffraction signal has been acquired through theta/2theta scans from 10 to 80° with 0.02° step, with an acquisition time of 1s/step.

2.3 Fixed-bed column set up

The FBC-CuO column consisted of a cylinder stainless steel cylinder (18 mm internal diameter (I.D.) × 200 mm height) filled with 140 g of CuO pellets. The use of millimetric CuO pellets allowed to respect the requirement of limiting the pressure drop inside a column (Metha and Hawley 1969) and preventing potential clogging problems. Two metal grids with a mesh smaller than the size of the CuO pellets were positioned at the inlet and the outlet of the column. FBC-CuO consists of a volume occupied by the solid CuO pellets (22 mL) and an empty bed volume (EBV, 29 mL) corresponding to an experimental porosity equal to 0.55. As shown in Fig. S1, the FBC-CuO was vertically oriented and silicone tubes were connected at both ends. The inlet at the bottom of the column was driven by a peristaltic pump (lab 2015, Shenchen, China) to control flow rates, and the outlet was at the top of the column. Three micro-valves were evenly located on the column evenly 5 cm for local sampling and accessed the internal

concentration profiles of the different components. All experiments were operated in upflow mode at a controlled flow rate.

2.4 Experimental procedures

2.4.1 Phenol degradation with FBC-CuO/PDS process

To have a thorough understanding of the working mode, phenol was selected as the probe compound. Tris buffer (20 mM) was used as the water matrix to maintain the neutral pH of the solution for all the experiments with phenol. As no adsorption or degradation of phenol by CuO alone were observed (Li et al. 2021), it was decided to start the experiments with a column filled with the phenol solution. Pure phenol solution (5 mg/L) flowed from a tank into the column with a 3 mL/min flow rate until the outlet concentration equal the inlet concentration. A uniform concentration of phenol inside the column represented the initial conditions of the degradation experiments. Experiments were systematically triggered by the addition of PDS to the phenol solution and a flow into the column according to the selected flow rate. From this starting point, the solution flow rate and the inlet phenol and PDS concentrations kept unchanged. Aliquots of treated water samples were collected at the predetermined time from the outlet and three valves. Samples were stored at 4 °C before analysis. The working mode of the phenol removal was expected to happen in a first phase in dynamic regime and followed by a second phase in permanent regime.

2.4.2 Antibiotics degradation with FBC-CuO and FBC-CuO/PDS processes

To evaluate the degradation performance of antibiotic micropollutants on the FBC-CuO column, 250 µg/L of AMX, CFX, OFX, SMX, and CLA, which have been commonly detected in urban wastewater, were spiked to DW and STWW from an activated sludge wastewater treatment plant, respectively. The physio-chemical properties of STWW are listed in Table S1. STWW was firstly filtered through a 200 µm sieve to remove the largest suspended solids and prevent the clogging problem.

Differently with phenol, the interaction between Cu(II) with some specific antibiotics was previously reported (Lapshin and Alekseev 2009; Chen et al. 2019). Thus, the starting point of the antibiotic degradation experiments was corresponding to the FBC-CuO filled with pure water. Firstly, the antibiotics mixture solution flowed through the column without PDS, then a constant inlet concentration of PDS was added in the inlet solution. Aliquots of treated water samples were collected at the predetermined time from the column outlet, and stored at 4 °C before analysis.

2.4.3 Pathogens inactivation with FBC-CuO and FBC-CuO/PDS processes

STWW was collected from the same activated sludge wastewater treatment plant and was also filtered through a 200 µm sieve before the disinfection experiment. To evaluate the disinfection performances and to comply with the EU Regulation 2020/741 of the European Parliament on minimum requirements for water reuse, *E. coli*, *Enterococcus*, *F-specific RNA bacteriophages*, and *spores of sulfite-reducing bacteria* were selected as the indicator of Gram-negative, Gram-positive bacteria, virus, and protozoa, respectively. The pathogenic indicators originally presented in wastewater were targeted to monitor.

It was checked that at ambient temperature PDS alone as no effect on the different indicators (Li et al. 2022). At the opposite, CuO alone, may interact and provide non-negligible disinfection effects (Ren et al. 2009; Suleiman et al. 2015; Li et al. 2022), especially when implemented in the form of nanoparticles. For this reason, disinfection experiments were operated as in the case of the experiments dedicated to antibiotic degradation. A first step corresponding to the flowing of the effluent through the FBC-CuO system without PDS. A second step corresponding to the flowing of the effluent at the same flow rate with a constant concentration of PDS at the inlet of the column.

The column was design to operate with flow rates of few mL/min to provide consistent residence times. Measurement of the four targeted pathogens needed to collect one liter of each sample. As a consequence, it was not possible to investigate the pathogens

inactivation process in dynamic regime due to the long sampling period, and the sampling was carried out in the both cases (with and without PDS) when the permanent regime was reached after at least 2 hours of operating.

To ensure the stable viability of pathogens, the effluents in the sterile water tanks at the inlet and outlet of the column were surrounded by ice pads. Samples were stored at 4 °C and pathogens analysis was conducted less than 24 h after sample collection.

2.5 Analytical methods

2.5.1 Quantification of phenol and PDS

Phenol concentrations were quantified by LC with a diode-array detector at $\lambda = 280$ nm using an Agilent ZORBAX Eclipse XDB C8 column (150 × 3 mm i.d., 3.5 μm particle size). The separation was performed using an isocratic mode of elution with a mobile phase composed of 0.1% formic acid in Milli-Q water and acetonitrile at a volume ratio of 50/50. The flow rate was set at 0.5 mL/min. The injection volume of each sample was 10 μL.

PDS was determined by using a UV-Vis spectrophotometer (Shimadzu, Japan). Briefly, the method already reported (Li et al. 2021) consisted in analyzing adsorption spectra of mixed solutions of 1 mL sample, 1 mL 60 mM $NaHCO_3$, and 1 mL 600 mM KI in a quartz cuvette at $\lambda = 352$ nm.

2.5.2 Quantification and transformation products analysis of antibiotics

Quantification of targeted antibiotics were analyzed by LC-HRMS composed of a Dionex Ultimate 3000 liquid chromatograph equipped with an electrospray source operated in the positive ionization mode and a Exactive Orbitrap mass spectrometer (Thermo Fisher Scientific, Les Ulis, France) operated in full scan MS (mass range m/z 50-900) and using an Agilent ZORBAX Eclipse XDB C18 plus column (150 × 2.1 mm i.d., 3.5 μm particle size). LC gradient of Milli-Q water with 1% acetonitrile and 0.1%

formic acid (solvent A) and acetonitrile with 1% Milli-Q water and 0.1% formic acid (solvent B) was as follow: 0-5 min, 95% A; 15-20 min, 5% A; 21-30 min, 95% A. The flow rate was 0.15 mL/min. The energy collisional dissociation was set to 20 eV and a drying gas temperature of 300 °C was used. The injection volume of each sample was 10 µL.

To gain insights into the targeted antibiotic degradation mechanisms of FBC-CuO alone, and FBC-CuO in presence of PDS, transformation products (TPs) of AMX, CFX, OFL, SMX, CLA were identified following a suspect screening workflow in LC-HRMS. The databases were made up of a list of possible TPs with their molecular formula and exact mass collected from the literature. The list of possible TPs of CFX, SMX, CLA were reported in the supplementary information in our previous study (Li et al. 2021). Possible TPs of AMX and OFL were listed in Table S2-S3.

2.5.3 Enumeration of pathogens

The NF EN ISO 9308-3 and NF EN ISO 7899-1 standard protocols were used to enumerate *E. Coli* and *Enterococcus* respectively. These methods are based on the culture of the bacteria in a liquid medium and the determination of the most probable number (MPN) according to the level of dilution. *F-specific RNA bacteriophages* were measured according to the ISO 10705-1 method. This method allows for a count on the agar medium of plaque-forming unit (PFU), corresponding to the number of viruses. The NF EN 26461-2 standard protocol was used to enumerate the colony-forming unit (CFU) of *spores of sulfite-reducing bacteria* after filtration and cultivation on a specific agar solid medium.

2.5.4 Cu(II) analysis

Cu(II) leached from CuO pellet was analyzed by inductively coupled plasma - optical emission spectrometry (ICP-OES) using an iCap Duo 7400 spectrometer (Thermo Fischer Scientific, Les Ulis, France) using the axial mode of detection at wavelength λ = 324.754 nm.

3. Results and discussion

3.1 Working mode of the CuO pellet fixed-bed column

As detailed in the section 2.4.1, before each degradation experiment, the column was charged with a pure phenol solution at a given concentration. Fig. 1a presents the breakthrough curve of the phenol at the outlet of the column in the case of a volume flow rate equal to 3 mL/min and an inlet concentration of phenol (C_{ph_i}) equal to 5 mg/L. The Reynolds number (Re) under flowing conditions was much smaller than 1, indicating a highly laminar flow regime in the column. The axial diffusion coefficient is estimated to be in the range of 2×10^{-6} m^2s^{-1} with the popular and simplified Chun and Wen (1968) empirical equation (Table S4) adapted to flowing conditions with $Re < 1$. As expected, and in agreement with the low value of the Peclet number (around 0.2), the shape of the breakthrough curve was characteristic of a plug-flow with an important axial dispersion resulting in an "S-curve". Finally, the theoretical phenol quantity calculated taking into account the EBV and the minor dead volumes at the inlet and the outlet of the column, was equal to the actual phenol quantity calculated from the breakthrough curve (around 0.14 mg), which further confirmed that there was no detectable adsorption of phenol at the surface of the CuO pellet and no scalable persistent interaction between this molecule and the CuO.

For the record, the initial time (t = 0) in Fig. 1b corresponds to a column with a uniform inlet and outlet phenol concentration ($C_{ph\_i} = C_{ph\_o} = 5$ mg/L) and without any trace of PDS but operating, from this moment with a volume flow of 3 mL/min, and inlet PDS (C_{PDS_i}) and phenol concentrations equal to 500 µM and 5 mg/L respectively. As expected, the column operated in two different regimes. The first dynamic regime corresponded to the establishment of the PDS and phenol concentration profiles in the fixed packed bed. During this phase, the concentrations of both species inside the column were the result of the coupling between the convective mass transport, mass diffusion of both species, kinetic of phenol removal, and kinetic of PDS consumption.

The breakthrough time of the PDS (Fig. 1b) was consistent with the one obtained in the case of phenol during the preliminary charge, and gave the limit between the dynamic and the permanent regime. It took at least 40 to 50 min for a completed establishment of the permanent regime, and then the concentrations of both species remained constant at the outlet. Their absolute values depended on the operating parameters of the column i.e., the volume flow rate and the inlet concentrations of phenol and PDS. For the selected conditions, phenol was almost complete removed but PDS was not fully consumed. Around 20% of the PDS at the inlet of the column remained at the outlet. After 60 min, the local concentrations of phenol and PDS were very stable at any position inside the column during the entire measurement period of several hours (Fig. 1c and d), which well confirmed the fully steady-state operation of the process. The profiles also clearly indicated that, for these particular operating conditions, the inlet concentration of the PDS was in excess. PDS remained at the outlet of the column while only half of the column was necessary to provide complete removal of the inlet phenol flux (Fig. 1c).

The performance of the FBC-CuO with 5 mg/L influent phenol and 3 mL/min flow rate was tested at varying influent PDS concentrations. Whatever were the working conditions, the two regimes were checked with a period necessary for the establishment of the quasi-static regime almost independent of the PDS inlet concentration (Fig. 2a and c). Obviously, PDS dosage was a major factor that determined the column performances. As expected, higher influent PDS concentration promoted the oxidative mechanisms and led to higher phenol removal efficiency and treatment capacity (Table 1). A twofold increase in the treatment capacity was observed when PDS concentration varying from 125 μM to 500 μM. With 125 μM at the inlet, there was no more PDS in the solution at an axial position between 5 and 10 cm (Fig. 2d). From this position, the concentration of the phenol remained constant (Fig. 2b). In the case of a too much low inlet PDS concentration, all the oxidant was consumed in the front part of the column,

leading to an unused bed length were no degradation of the pollutant happened. On the contrary, a too high inlet PDS concentration was inefficient and counterproductive. No improvement of the treatment capacity was detected when PDS inlet concentration was increased from 500 µM to 1000 µM (Table 1) while a useless release of PDS at the outlet happened (Fig. 2c). As in the previous case but for a different reason, a too high dosage of PDS (1000 µM) also led to an unused bed length. In the first part of the column, the high removal kinetic of phenol linked to the high level of PDS concentration led to complete removal of the phenol between 5 and 10 cm (Fig. 2b). For these particular conditions, a mass flow of 3 mL/min and an inlet concentration of phenol of 5 mg/L, an inlet concentration of PDS between 250 and 500 µM would have probably been the optimal value to achieve no PDS release at the outlet with a total phenol removal thanks to an optimal use of the length of the column.

Table 1. Removal efficiency and treatment capacity of phenol by FBC-CuO/PDS system with varying influent PDS concentration.

Flow rate (mL/min)	C_{ph_i} (mg/L)	C_{PDS_i} (µM)	Removal efficiency (%)	Treatment capacity of phenol (µg/min)
3	5	0	0	0
		125	46	7.41
		250	81	12.36
		500	95	14.14
		1000	97	14.55

Even if only specific operating conditions were provided for a particular column design, this qualitative analysis clearly demonstrated that the control of the FBC-CuO process can easily be achieved by controlling and regulating the inlet oxidant concentration. This was further confirmed by the results conducted within the objective of studying the effects of the phenol inlet concentration, the volume flow, and presented as supplementary material (Fig. S2-S3).

3.2 Degradation of antibiotics

In the case of trials carried out in distilled water (Fig. 3a and 3b), as detailed in the section devoted to the experimental procedure, in a first step, a mixture of AMX (penicillin), CFX (cephalosporin), OFL (quinolone), SMX (sulfonamide), and CLA (macrolide) in DW flowed through FBC-CuO at a flow rate of 1.5 mL/min. Different trends were noticed (Fig. 3a). In this case, corresponding to a more complex mixture with probably competitive phenomena between the surface of CuO and some of the pharmaceutical compounds, the breakthrough times of each species were not uniform. However, only a few tens of minutes separated the breakthrough times of SMX and CLA, the two species with a fully breakthrough at the outlet of the column which happened around 1 h. This order of magnitude was in agreement with a breakthrough derived from the resident time (35 min in the working conditions) combined with significant diffusional transport phenomena. CFX and OFX corresponded to an intermediate behavior. Breakthrough happened but saturation of the column was never reached. The outlet concentrations of both species kept lower than the inlet concentrations, even after a very long operating period (18 h) and a permanent regime definitively established as clearly indicated by the concentration profiles of the species. Finally, whatever was the operating period, AMX was always undetectable at the outlet of FBC-CuO. AMX, CFX, and OFL were completely or partially removed by FBC-CuO alone (Table 2).

Hydrolysis of β-lactam antibiotic family can be a significant degradation pathway in the environment, but it usually takes 5.3-27 days at pH 7 and 25°C (Mitchell et al. 2014). It could not be the main degradation pathway in this study. Adsorption mechanism was excluded because of the very low specific surface area of CuO (Li et al. 2021). Another possible mechanism may be the complexation of Cu(II) with β-lactam antibiotics (AMX and CFX) and fluoroquinolones (OFL). AMX and CFX contain the carboxylic, amide, and amino groups, which resemble dipeptides in acid-base and ligand properties, and exist as anions at neutral pH, then subsequently interact with Cu(II) (Lapshin et al.

2009; Lipunova et al. 2009; Chen et al. 2019). Transformation products of AMX, CFX, and OFL in FBC-CuO were identified following a suspect screening workflow in LC-HRMS. For this purpose, a database was made up of a list of possible TPs with their molecular formula, exact mass, and structure (see Table S1 and S2, and SI of previously work by our group (Li et al. 2021)). This list was established from a literature search of TPs. TPs with intensities lower than 1 $x10^4$ cps, signal to noise ratios lower than 10, isotopic ratio higher than 10%, and mass accuracy errors higher than 5 ppm were discarded. The identified TPs of CFX, AMX, and OFL were shown from Fig. S4, S5, S6 representatively. The transformation pathways of AMX, CFX, and OFL in FBC-CuO were tentatively elucidated (Fig. S7). The formation of TPs most likely through a one electron transfer from the antibiotic to the metal in the complex, demonstrated the evidence of the degradation of AMX, CFX and OFL by FBC-CuO alone. Actually, a detail study of transformation mechanims were outside the scope of this work. However, the compounds which underwent removal (AMX, CFX and OFX) were those which form a complex with copper. That's why we assumed that copper played a role in their elimination may be through one electron oxidation processes or by accelerating the hydrolysis of the lactam ring. But these mechanisms were not demonstrated in this work and will deserve more research. In case of AMX, the direct reaction between AMX and singlet oxygen could not be discarded as previously reported (Zhao et al., 2013). However, the formation of singlet oxygen was not demonstrated in FBC-CuO system and could be only anticipated in presence of PDS.

After 18 h of operation, the column was in permanent regime, 500 µM PDS was added to the inlet water tank. As shown in Fig. 3b, the addition of PDS systematically and significantly enhanced the degradation of the antibiotics. The residual outlet concentration of CFX and OFL were rapidly removed. The presence of PDS was also the necessary condition for a partial but significant, removal of SMX and CLA. CFX and OFL were completely degraded after 30-40 min. 51 ± 2% of SMX and 34 ± 1% of

CLA were removed in the tested operating conditions when the quasi-permanent regime was reached.

In addition to DW, the removal efficiency of target antibiotics mixture in the actual wastewater operating under the same conditions was also evaluated, as shown in Fig. 4c and 4d. The degradation tendency of target antibiotics in DW and STWW was the same, however, the removal efficiency of targeted antibiotics decreased under the influence of various competitive components in the STWW (Fig. 3 and Table 2). For the first stage of FBC-CuO, the dissolved organic matter and anions (e.g. sulfate anions) in STWW could interact with Cu(II) or adsorbed on the CuO, resulting in less available activated sites on the CuO surface, and limited Cu(II) complexation with targeted antibiotics (Fig. 3a and c). For the second stage, less PDS could interact with CuO, resulting in less PDS consumption (Fig. S8), less reactive species production, and lower degradation efficiency for all targeted antibiotics (Fig. 3b and d). According to our previous work dealing with mechanisms of activation of persulfate in CuO/PDS system (Li et al, 2021), PDS activation is launched by the interaction between the positively charged CuO and the negatively charged PDS. In this first work, it was shown that anions such as sulfate anions and DOM can preclude or limit the interaction between CuO/PDS resulting in a decrease in efficiency. Sulfate anions and negatively charge DOM most likely interacted with positively charged CuO competing with antibiotics and/or PDS for interaction at CuO surface.

Table 2. Removal efficiency (RE) of selected antibiotics by FBC-CuO alone and FBC-CuO/PDS in DW and STWW.

RE	DW		STWW	
	FBC-CuO	FBC-CuO/PDS	FBC-CuO	FBC-CuO/PDS
AMX (%)	100	100	59 ± 3	100
CFX (%)	70 ± 2	100	25 ± 1	52 ± 2
OFX (%)	34 ± 1	100	31 ± 1	90 ± 2
SMX (%)	0	51 ± 2	0	20 ± 1
CLA (%)	0	34 ± 1	0	20 ± 1

3.3 Pathogens inactivation

In a first step, the STWW was flowed through the FBC-CuO at a flow rate equal to 3 mL/min. After 2 h of operation, the working mode of FBC-CuO was expected to reach the permanent regime. From this moment, the sampling at the outlet of the column started to collect the necessary 1 L effluent for pathogens analysis. Comparison between the inlet and the outlet pathogens concentrations is provided in Fig. 4a. The abundances in secondary-treated effluent samples before treatment were 5.3 ± 0.1 $\log_{10}$ MPN/100 mL of *E. coli*, 4.6 ± 0.1 $\log_{10}$ MPN/100 mL of *Enterococcus*, 4.0 ± 0.1 $\log_{10}$ PFU/100 mL of *F-specific RNA bacteriophages*, and 3.5 ± 0.2 $\log_{10}$ CFU/100 mL of *spores of sulfite-reducing bacteria* and are comparable to the values found in the literature (Mandilara et al. 2006; Haramoto et al. 2015). When the effluent simply flowed through FBC-CuO without PDS, the reduction of bacteria and parasite was very limited for *E. coli* (0.2 log), *Enterococcus* (0.2 log), and *spores of sulfite-reducing bacteria* (0.3 log), but for virus, a considerable reduction of *F-specific RNA bacteriophages* (2.7 log) was observed. This was most likely a consequence of the presence at low concentration of Cu(II) due to leaching from the surface of CuO pellets. As detailed in the next section, this species, which presents well known biocidal characteristics, was identified by suitable methods in the effluent at the column outlet.

In a similar way to the test carried out on antibiotics, the second step was initiated by the addition of 500 µM of PDS to the inlet water tank and sampling started when the permanent regime was reached. Prior to this experiment, and as already demonstrated (Li et al. 2022) it was checked that PDS alone at ambient temperature had no measurable effects on the abundances of pathogens. When the effluent flowed through FBC-CuO with PDS, the reduction of 3 of the 4 pathogens indicators significantly increased. *E. coli* (3.6 log) and *F-specific RNA bacteriophages* (3.8 log) were respectively removed up to or just above the limit of detection. *Enterococcus* was also significantly inactivated (1.3 log). However, the reduction of *spores of sulfite-reducing bacteria* (0.2 log, 38% abatement), the indicator representative of the parasite, was still

limited. Such pathogens are well identified in the literature as extremely difficult to inactivate and resistant to disinfection processes, such as chlorination (Shields et al. 2008) and UV (Hijnen et al. 2006), but can alternatively be removed by low cost slow sand filtration system (Timms et al. 1995).

Pathogens were ranked as *E. coli* and *F-specific RNA bacteriophages* > *Enterococcus* > *spores of sulfite-reducing bacteria* according to the treatment effectiveness criteria, and was fully confirmed by the tests carried out at different flow rates (Fig. 4b). Spores were not inactivated by a process based on the combination of PDS and FBC-CuO, whatever the operating conditions. At the opposite, the evolution of conversion rates for the other three treatment-sensitive pathogens attested of the influence of operating conditions. In such a process based on the coupling between kinetic of inactivation and mass transport, an increase of the residence time almost systematically resulted in an increase of the conversion rates. Finally, the triplicate performed with a flow rate equal for 1.5 mL/min brought to light the well-known uncertainty linked to the quantification of any pathogens populations, especially in the case of non-stabilized and non-controlled effluents such as STWW.

3.4 Stability of FBC-CuO

One of the essential characteristics for a catalyst to be a candidate for application in large-scale wastewater treatment is its stability and ability to maintain catalytic activity during long period of operation. Consequently, possible structural changes of the CuO pellet were evaluated by analyzing the catalyst recovered after all the measurement campaigns presented using SEM and X-ray diffractograms.

The SEM images of the surface of the millimetric CuO pellets were analyzed before and after the campaigns. The Fig. 5a and 5b highlighted that the surface was made off aggregates. A slight agglomeration of particles after treatment was observed, which may be due to the mechanism of PDS activation by CuO. This reaction that involved, during one step, an upper copper oxidation level, the cupryl ion (Li et al 2021), possibly

led to additional local corrosion of CuO favorable to a slow and slight agglomeration phenomenon. However, in this study, no significant difference was obtained, with only slight changes from 623 ± 74 nm before treatment to 700 ± 30 nm after treatment, which indicated the good stability of surface morphology of CuO pellets.

The XRD diffractogram before and after treatment (Fig. 5c) shows well-defined and intense diffraction peaks located at the positions 2Θ = 32.66, 35.63, 38.78, 46.37, 48.92, 53.61, 58.37, 61.70, 65.95, 66.39, 68.17 and 72.51. These peaks correspond to the monoclinic structure of CuO (Asbrink et al. 1991; Angi et al. 2014; Lanje et al. 2017). Lattice parameters were calculated and are a = 4.70 Å, b = 3.42 Å, c = 5.10 Å. The intensities, positions of the peaks and the lattice parameters are in good agreement with the reported values JCPDS file N^{o}. 96-901-6058.

During disinfection trials in presence of PDS, stability of the catalyst was assessed against the leached concentration of Cu measured in solution by ICP-AES after a filtration step on 0.45 µm cellulose filters (Fig. 5d). Even if non negligible, the Cu leaching from CuO was limited and far less than that of 2 mg/L which is required by environmental quality standards for surface water and by drinking water regulations (WHO 2004).

Therefore, the results showed that the material presented phase purity and stability before and after treatment. The good stability and catalytic efficiency of CuO pellet at near neutral pH, make this system promising for application.

4. Conclusions

PDS activation by using CuO pellet as heterogeneous catalyst in a fixed-bed column was applied for wastewater decontamination and disinfection. The first set of experiments performed with a simple solution of phenol in distilled water have demonstrated that this process, as any process based on the flowing of a reactive

mixture through a fixed packed bed was sensitive to operating conditions, especially for flow rate and influent PDS concentration. FBC-CuO alone presented significant removal performance on ß-lactam and fluoroquinolones antibiotics through Cu(II) complexation and degradation. But FBC-CuO alone demonstrated limited disinfection performance. The combination of PDS with FBC-CuO was the necessary condition for the degradation of SMX and CLA, not only improving the antibiotics degradation, but also greatly enhancing the pathogens inactivation performances, excepted for *spores of sulfite-reducing bacteria*, the indicator selected as representative of the parasites. It is suggested that after the oxidative treatment, post-treatment by low-cost slow sand filtration or ionized clay filtration, well adapted to parasites separation because of their high characteristic size, may overcome the main limitations of this process. The characterization comparison of CuO pellet before and after treatment and the measurement of Cu(II) leaching demonstrated the excellent stability and reusability of the CuO pellets.

Overall, it was shown that combination of PDS with FBC-CuO constitutes an efficient and promising treatment option for the removal of micropollutants and microorganisms from urban wastewater effluents.

Statements & Declarations

Authors contributions - Chan Li , Formal analysis – writing – original draft, review & editing ; Nayara de Melo Costa Serge and Raquel Fernandes Pupo Nogueire, Experimental data interpretation. Serge Chiron, and Vincent Goetz, Conceptualization – writing, review & editing.

Funding - This research was financially supported by the Water Joint Programming Initiative (JPI) through the research project IDOUM - Innovative Decentralized and low cost treatment systems for Optimal Urban wastewater Management and in part by

the MITI CNRS/IRD program through the research project FREE - AC/CuO Filter Regenerated by solar Energy for water rEuse. Chan Li thanks the Occitanie Region for her PhD grant. Nayara de Melo Costa Serge thanks the São Paulo Research Foundation (FAPESP, grants #2019/24642-0 and #2018/17517-0) for her financial support and a doctoral scholarship.

Competing Interests - The authors declare that they have no known competing financial interests or personal relationships that could have appeared to influence the work reported in this paper.

Availability of data and materials

The datasets used and analyzed during the current study are available from the corresponding author on reasonable request.

Ethic approval

Not applicable.

Consent to participate

All authors have given consent to their contribution.

Consent for publication

All authors have agreed with the content and all have given consent to publish.

References

Andrigo P., Bagatin R., Pagani G. (1999) Fixed bed reactors. Catalysis Today. 52: 197-221. https://doi.org/10.1016/S0920-5861(99)00076-0.

Angi A., Sanli D., Erkey C., Birer Ö. (2014) Catalytic activity of copper (II) oxide prepared via ultrasound assisted Fenton-like reaction. Ultrason. Sonochem. 25: 854–859. https://doi.org/10.1016/j.ultsonch.2013.09.006.

Asbrink S. and Waskowska A. (1991) CuO: X-ray single-crystal structure determination at 196 K and room temperature. J. Phys. Condens. Matter. 3: 8173–8180. https://doi.org/10.1088/0953-8984/3/42/012.

Brienza M., Nir S., Plantard G., Goetz V., Chiron S. (2019) Combining micelle-clay sorption to solar photo fenton processes for domestic wastewater treatment. Env. Sci. and Pollution Research. 26 :18971-18978, https://doi.org/10.1007/s11356-018-2491-3.

Chen J., Zhou X., Sun P., Zhang Y., Huang C.H. (2019) Complexation Enhances Cu(II)-Activated Peroxydisulfate: A Novel Activation Mechanism and Cu(III) Contribution. Environ. Sci. Technol. 53: 11774–11782. https://doi.org/10.1021/acs.est.9b03873.

Chen Y.D., Duan X., Zhou X., Wang R., Wang S., Ren N.Q., Ho S.H. (2021) Advanced oxidation processes for water disinfection: Features, mechanisms and prospects. Chem. Eng. J. 409: 128207. https://doi.org/10.1016/j.cej.2020.128207.

Cho Y.C., Lin R.Y., Lin Y.P. (2020) Degradation of 2,4-dichlorophenol by CuO-activated peroxydisulfate: Importance of surface-bound radicals and reaction kinetics. Sci. Total Environ. 699: 134379. https://doi.org/10.1016/j.scitotenv.2019.134379.

Chung S.F. and Wen C.Y. (1968) Longitudinal dispersion of liquid flowing through fixed and fluidized beds. AIChE J. 14: 857–866. https://doi.org/10.1002/aic.690140608.

Crittenden J.C., R. Rhodes Trussell R., Hand D.W., Howe K.J., Tchobanoglous G. (2012) Water Treatment Principles and Design (third edition). John Wiley & Sons, Inc.

Ding Y., Fu L., Peng X., Lei M., Wang C., Jiang J (2022) Copper catalysts for radical and nonradical persulfate based advanced oxidation processes: Certainties and uncertainties. Chem. Eng. J. 427: 131776. https://doi.org/10.1016/j.cej.2021.131776.

Du X., Zhang Y., Hussain I., Huang S., Huang W. (2017) Insight into reactive oxygen species in persulfate activation with copper oxide: Activated persulfate and trace radicals. Chem. Eng. J. 313: 1023–1032. https://doi.org/10.1016/j.cej.2016.10.138.

Gmurek M., Horn H., Majewsky M. (2015) Phototransformation of sulfamethoxazole under simulated sunlight: Transformation products and their antibacterial activity toward Vibrio fischeri. Sci. Total Environ. 538: 58–63. https://doi.org/10.1016/j.scitotenv.2015.08.014.

Haramoto E., Fujino S., Otagiri M. (2015) Distinct behaviors of infectious F-specific RNA coliphage genogroups at a wastewater treatment plant. Sci. Total Environ. 520: 32–38. https://doi.org/10.1016/j.scitotenv.2015.03.034.

Hijnen W.A.M., Beerendonk E.F., Medema G.J. (2006) Inactivation credit of UV radiation for viruses, bacteria and protozoan (oo)cysts in water: A review. Water Res. 40: 3–22. https://doi.org/10.1016/j.watres.2005.10.030.

Hirte K., Seiwert B., Schürmann G., Reemtsma T. (2016) New hydrolysis products of the beta-lactam antibiotic amoxicillin, their pH-dependent formation and search in

587 municipal wastewater.Water Res. 88: 880–888.
588 https://doi.org/10.1016/j.watres.2015.11.028.

589 Lanje A.S., Sharma S.J., Pode R.B. (2017) Synthesis and Characterization of Copper
590 Oxide Nanoparticles. Int. J. Adv. Eng. Res. Dev. 04:
591 https://doi.org/10.21090/ijaerd.ncn01.

592 Lapshin S. V., Alekseev V.G. (2009) Copper(II) complexation with ampicillin,
593 amoxicillin, and cephalexin. Russ. J. Inorg. Chem. 54: 1066–1069.
594 https://doi.org/10.1134/S0036023609070122.

595 Lee J., Von Gunten U., Kim J.H. (2020) Persulfate-Based Advanced Oxidation:
596 Critical Assessment of Opportunities and Roadblocks. Environ. Sci. Technol. 54:
597 3064–3081. https://doi.org/10.1021/acs.est.9b07082.

598 Levenspiel O. (1972), Chemical reaction engineering. John Wiley & Sons, Inc

599 Li C., Goetz V., Chiron S. (2021) Peroxydisulfate activation process on copper oxide:
600 Cu(III) as the predominant selective intermediate oxidant for phenol and waterborne
601 antibiotics removal. J. Environ. Chem. Eng. 9: 105145.
602 https://doi.org/10.1016/j.jece.2021.105145.

603 Li C., Goetz V., Chiron S. (2022) Copper oxide/peroxydisulfate system for urban
604 wastewater disinfection: Performances, reactive species, and antibiotic resistance
605 genes removal. Sci. Total Environ. 806: 150768.
606 https://doi.org/10.1016/j.scitotenv.2021.150768.

607 Liang H.Y., Zhang Y.Q., Bin Huang S., Hussain I. (2013) Oxidative degradation of p-
608 chloroaniline by copper oxidate activated persulfate. Chem. Eng. J. 218: 384–391.
609 https://doi.org/10.1016/j.cej.2012.11.093.

610 Lipunova G.N., Nosova E. V., Charushin V.N. (2009) Metallocomplexes of
611 fluoroquinolonecarboxylic acids. Russ. J. Gen. Chem. 79: 2753–2766.
612 https://doi.org/10.1134/S1070363209120342.

613 Luo H., Zeng Y., He D., Pan X. (2021) Application of iron-based materials in
614 heterogeneous advanced oxidation processes for wastewater treatment: A review.
615 Chem. Eng. J. 407: 127191. https://doi.org/10.1016/j.cej.2020.127191.

616 Mandilara G.D., Smeti E.M., Mavridou A.T., Lambiri M.P., Vatopoulos A.C., Rigas
617 F.P. (2006) Correlation between bacterial indicators and bacteriophages in sewage
618 and sludge. FEMS Microbiol. Lett. 263: 119–126. https://doi.org/10.1111/j.1574-
619 6968.2006.00414.x.

620 Mazurkow J.M., Yüzbasi N.S., Domagala K.W., Pfeiffer S., Kata D., Graule T.
621 (2020) Nano-Sized Copper (Oxide) on Alumina Granules for Water Filtration: Effect
622 of Copper Oxidation State on Virus Removal Performance. Environ. Sci. Technol. 54:
623 1214–1222. https://doi.org/10.1021/acs.est.9b05211.

624 Mehta D. and Hawley M.C. (1969) Wall effect in packed columns. Ind. Eng. Chem.
625 Process Des. Dev. 8: 280–282. https://doi.org/10.1021/i260030a021.

626 Mitchell S.M., Ullman J.L., Teel A.L., Watts R.J. (2014) PH and temperature effects
627 on the hydrolysis of three β-lactam antibiotics: Ampicillin, cefalotin and cefoxitin.
628 Sci. Total Environ. 466–467: 547–555.
629 https://doi.org/10.1016/j.scitotenv.2013.06.027.

630 Obra Jiménez I. , Giannakis S., Grandjean D., Breider F., Grunauer G., Casas López
631 J.L., Sánchez Pérez J.A., Pulgarin C. (2020) Unfolding the action mode of light and
632 homogeneous vs. heterogeneous photo-Fenton in bacteria disinfection and concurrent
633 elimination of micropollutants in urban wastewater, mediated by iron oxides in
634 Raceway Pond Reactors. Appl. Catal. B Environ. 263: 118158.
635 https://doi.org/10.1016/j.apcatb.2019.118158.

636 Poirier-Larabie S., P.A. Segura P.A., Gagnon C. (2016) Degradation of the
637 pharmaceuticals diclofenac and sulfamethoxazole and their transformation products
638 under controlled environmental conditions. Sci. Total Environ. 557–558: 257–267.
639 https://doi.org/10.1016/j.scitotenv.2016.03.057.

640 Qian Y., Xue G., Chen J., Luo J., Zhou X., Gao P., Wang Q. (2018) Oxidation of
641 cefalexin by thermally activated persulfate: Kinetics, products, and antibacterial
642 activity change. J. Hazard. Mater. 354: 153–160.
643 https://doi.org/10.1016/j.jhazmat.2018.05.004.

644 Ren G., Hu D., Cheng E.W.C., Vargas-Reus M.A., Reip P., Allaker R.P. (2009)
645 Characterisation of copper oxide nanoparticles for antimicrobial applications. Int. J.
646 Antimicrob. Agents. 33: 587–590. https://doi.org/10.1016/j.ijantimicag.2008.12.004.

647 Shields J.M., Hill V.R., Arrowood M.J., Beach M.J. (2008) Inactivation of
648 Cryptosporidium parvum under chlorinated recreational water conditions. J. Water
649 Health. 6: 513–520. https://doi.org/10.2166/wh.2008.068.

650 Schönfeld W., Knöller J., Bremm K.D., Dahlhoff A., Weber B., König W. (1986)
651 Determination of Ciprofloxacine, Norfloxacine, and Ofloxacine by High Performance
652 Liquid Chromatography, Zentralblatt Fur Bakteriol. Mikrobiol. Und Hyg. - Abt. 1
653 Orig. A. 261: 338–344. https://doi.org/10.1016/S0176-6724(86)80051-7.

654 Senta I., Krizman-Matasic I., Terzic S., Ahel M. (2017) Comprehensive determination
655 of macrolide antibiotics, their synthesis intermediates and transformation products in
656 wastewater effluents and ambient waters by liquid chromatography–tandem mass
657 spectrometry. J. Chromatogr. A. 1509: 60–68.
658 https://doi.org/10.1016/j.chroma.2017.06.005.

659 Suleiman M., Mousa M., Hussein A.I.A.A. (2015) Wastewater disinfection by
660 synthesized copper oxide nanoparticles stabilized with surfactant. J. Mater. Environ.
661 Sci. 6: 1924–1937.

662 Rizzo L., Gernjak W., Krzeminski P., Malato S., McArdell C.S., Perez J.A.S., Schaar
663 H., Fatta-Kassinos D. (2020) Best available technologies and treatment trains to
664 address current challenges in urban wastewater reuse for irrigation of crops in EU
665 countries. Sci. Total Environ. 710: 136312.
666 https://doi.org/10.1016/j.scitotenv.2019.136312.

667 Ternes T.A., Prasse C., Eversloh C.L., Knopp G., Cornel P., Schulte-Oehlmann U.,
668 Schwartz T., Alexander J., Seitz W., Coors A., Oehlmann J. (2017) Integrated
669 Evaluation Concept to Assess the Efficacy of Advanced Wastewater Treatment
670 Processes for the Elimination of Micropollutants and Pathogens. Environ. Sci.
671 Technol. 51: 308–319. https://doi.org/10.1021/acs.est.6b04855.

672 Timms S., Slade J.S., Fricker C.R. (1995) Removal of Cryptosporidium by slow sand
673 filtration. Water Sci. Technol. 31: 81–84. https://doi.org/10.1016/0273-
674 1223(95)00245-I.

675 Wacławek S., Lutze H.V., Grübel K., Padil V.V.T., Černík M., Dionysiou D.D.
676 (2017) Chemistry of persulfates in water and wastewater treatment: A review. Chem.
677 Eng. J. 330: 44–62. https://doi.org/10.1016/j.cej.2017.07.132.

678 Wang J., Chu L., Wojnárovits L., Takács L. (2020) Occurrence and fate of antibiotics,
679 antibiotic resistant genes (ARGs) and antibiotic resistant bacteria (ARB) in municipal
680 wastewater treatment plant: An overview. Sci. Total Environ. 744: 140997.
681 https://doi.org/10.1016/j.scitotenv.2020.140997.

682 Wang J. and Wang S. (2018) Activation of persulfate (PS) and peroxymonosulfate
683 (PMS) and application for the degradation of emerging contaminants. Chem. Eng. J.
684 334: 1502–1517. https://doi.org/10.1016/j.cej.2017.11.059.

685 WHO (2004) Copper in drinking water, Background document for development of
686 WHO guidelines for drinking-water quality.
687 https://www.who.int/water_sanitation_health/dwq/chemicals/copper.pdf.

688 Yan J., Lei M., Zhu L., Anjum M.N., Zou J., Tang H. (2011) Degradation of
689 sulfamonomethoxine with Fe3O4 magnetic nanoparticles as heterogeneous activator
690 of persulfate. J. Hazard. Mater. 186: 1398–1404.
691 https://doi.org/10.1016/j.jhazmat.2010.12.017.

692

693 Zhao Q., Feng L., Cheng X., Chen C., Zhang L. (2013) Photodegradation of
694 amoxicillin in aqueous solution under simulated irradiation: influencing factors and
695 mechanisms. Water Sci. Technol., 67: 1605-1611.
696 https://doi.org/10.2166/wst.2013.033.

697 Zhang T., Chen Y., Wang Y., Le Roux J., Yang Y., Croué J.P. (2014) Efficient
698 peroxydisulfate activation process not relying on sulfate radical generation for water

699 pollutant degradation. Environ. Sci. Technol. 48: 5868–5875.
700 https://doi.org/10.1021/es501218f.

701 Zhou C.S., Wu J.W., Dong L.L., Liu B.F., Xing D.F., Yang S.S., Wu X.K., Wang Q.,
702 Fan J.N., Feng L.P., Cao G.L. (2020) Removal of antibiotic resistant bacteria and
703 antibiotic resistance genes in wastewater effluent by UV-activated persulfate. J.
704 Hazard. Mater. 388: 122070. https://doi.org/10.1016/j.jhazmat.2020.122070.

Figures capation

Fig. 1. (a) Breakthrough curve of phenol in FBC-CuO; (b) phenol and PDS concentration profiles as a function of the time at the outlet of FBC-CuO; internal (c) phenol and (d) PDS concentration profiles in FBC-CuO. C_{ph_i} = 5 mg/L, C_{PDS_i} = 500 µM, flow rate = 3 mL/min.

Fig. 2. The effect of different inlet PDS concentrations on outlet concentration profiles as a function of the time for (a) phenol and (c) PDS; on internal profiles when permanent regimes were reached for (b) phenol and (d) PDS. C_{PDS_i} = 125,250, 500, and 1000 µM, C_{ph_i} = 5 mg/L, flow rate = 3 mL/min.

Fig. 3. Degradation of target antibiotics in DW and STWW by FBC-CuO alone: (a), (c); and by FBC-CuO/PDS: (b), (d). $C_{AMX\_i} = C_{CFX\_i} = C_{OFL\_i} = C_{SMX\_i} = C_{CLA\_i}$ = 250 µg/L, C_{PDS_i} = 500 µM, flow rate = 1.5 mL/min.

Fig. 4. Pathogens enumerations in STWW before treatment at the inlet (BT) and after treatment at the outlet (AT) at a flow rate equal to 3 mL/min by FBC-CuO without and with PDS at a concentration C_{PDS_i} = 500 µM (a), with PDS, same concentration and flow rates equal to 1.5, 3, and 9 mL/min. For 1.5 mL/min, triplicates were carried out and measurements variability are shown (for values above LOF). Note: * represents MPN for E. coli and Enterococcus, PFU for F-specific RNA bacteriophages, and CFU for spores of sulfite-reducing bacteria.

Fig. 5. SEM images of CuO pellet (a) before and (b) after treatment; (c) X-ray diffractograms of CuO pellet before and after treatment; (d) copper leaching at the outlet of the FBC-CuO in presence of PDS after 1 h and 4 h of flowing, C_{PDS_i} = 500 µM, flow rate = 1.5 mL/min.

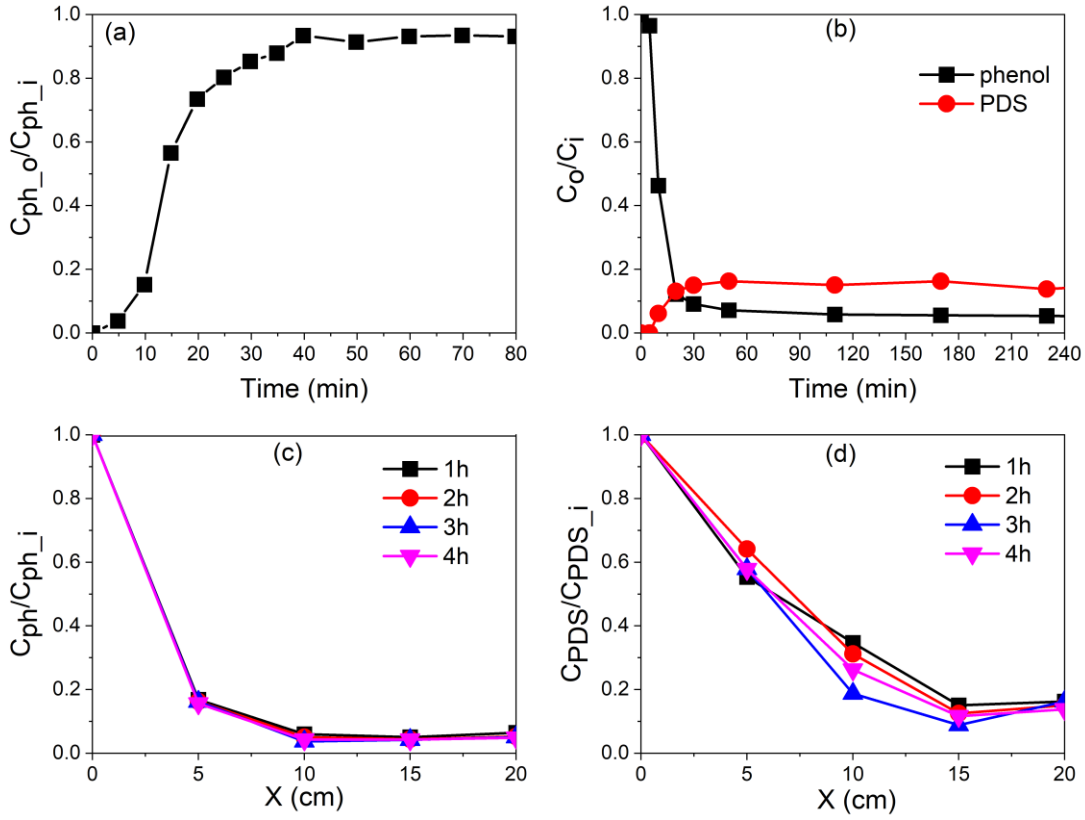
(a)
C_{ph_o}/C_{ph_i}
Time (min)
(b)
phenol
PDS
C_o/C_i
Time (min)
(c)
1h
2h
3h
4h
C_{ph}/C_{ph_i}
X (cm)
(d)
1h
2h
3h
4h
C_{PDS}/C_{PDS_i}
X (cm)

Fig. 1

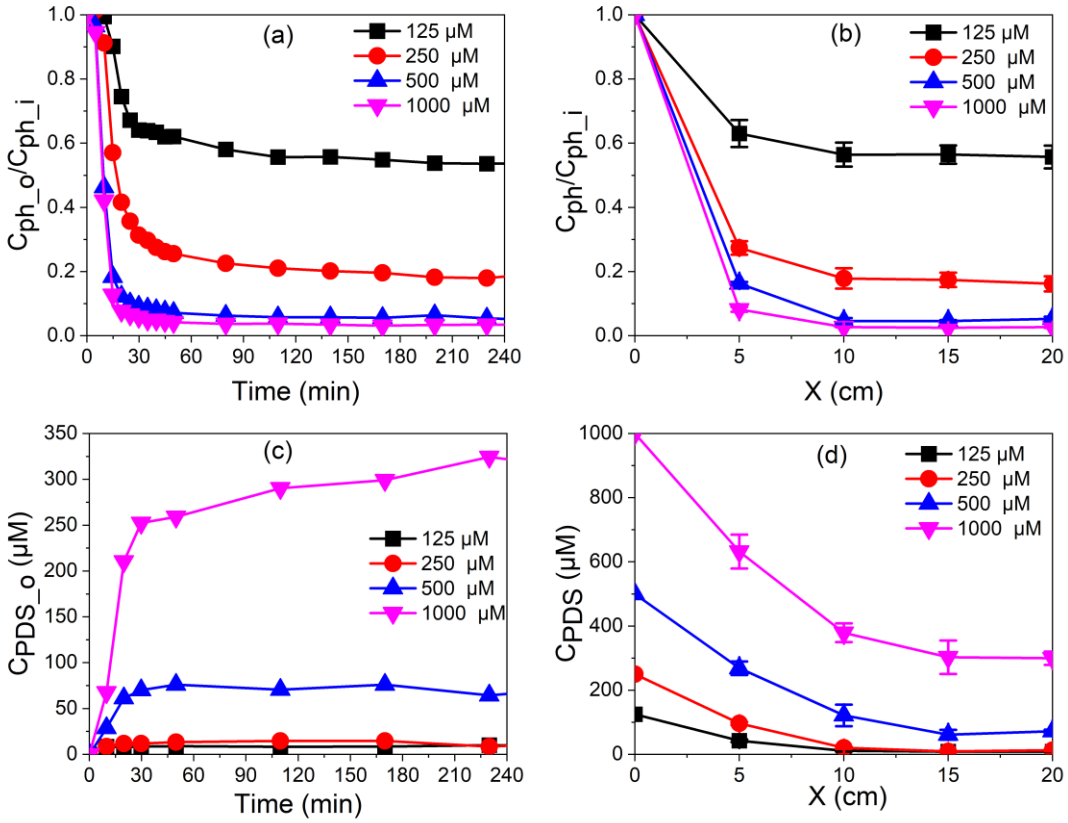
(a)
125 μM
250 μM
500 μM
1000 μM
Cph_o/Cph_i
Time (min)
(b)
Cph/Cph_i
X (cm)
(c)
CPDS_o (μM)
(d)
CPDS (μM)

Fig.2

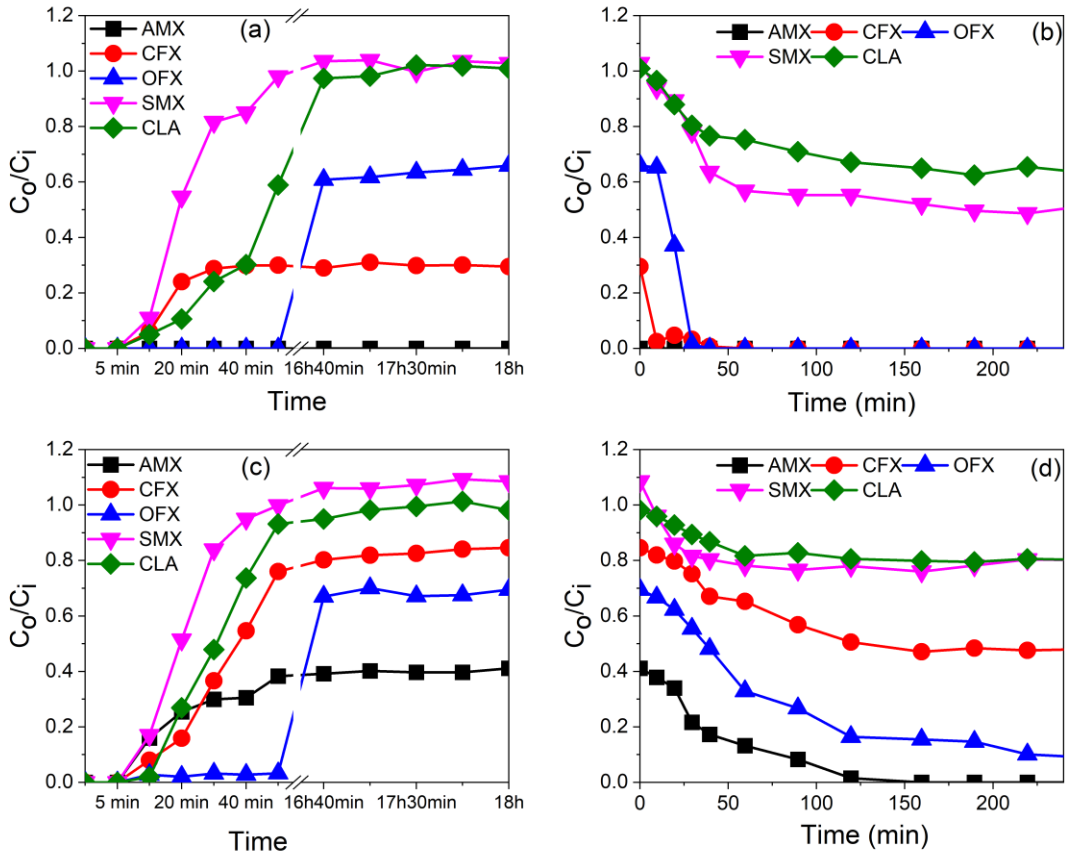
(a)
AMX
CFX
OFX
SMX
CLA
C_O/C_i
5 min
20 min
40 min
16h40min
17h30min
18h
Time
(b)
Time (min)
(c)
(d)

Fig. 3

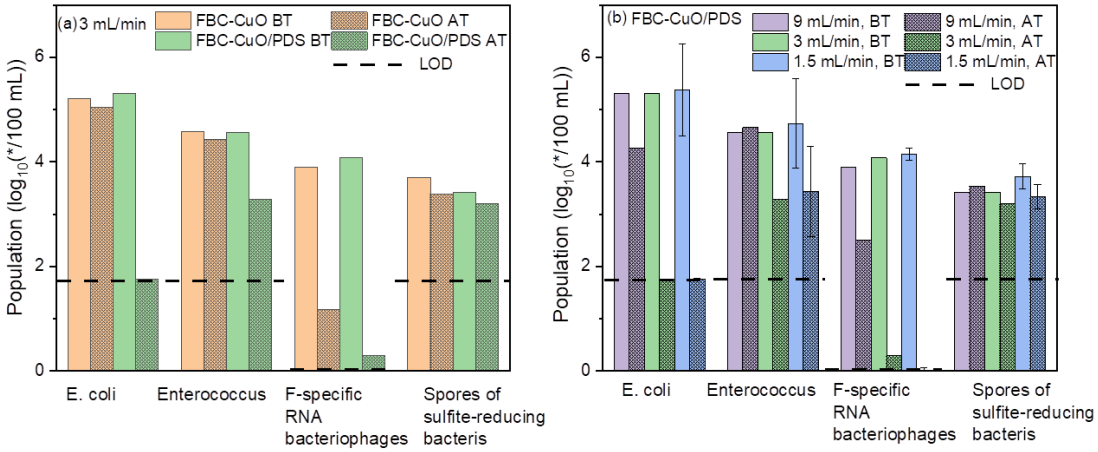

759

760 Fig. 4

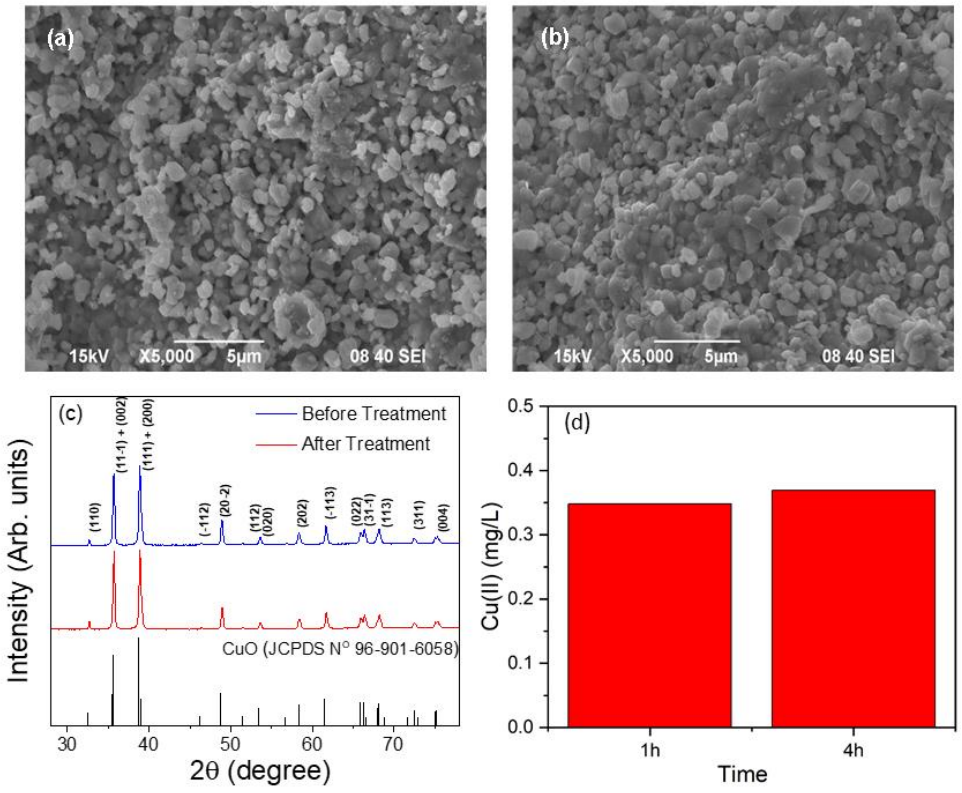

761

762 Fig. 5